Interface scattering in polycrystalline thermoelectrics

Adrian Popescu[1,2] and Paul M. Haney[1]
[1] *Center for Nanoscale Science and Technology, National Institute of Standards and Technology, Gaithersburg, Maryland 20899-6202, USA*
[2] *Maryland NanoCenter, University of Maryland, College Park, MD 20742, USA*

We study the effect of electron and phonon interface scattering on the thermoelectric properties of disordered, polycrystalline materials (with grain sizes larger than electron and phonons' mean free path). Interface scattering of electrons is treated with a Landauer approach, while that of phonons is treated with the diffuse mismatch model. The interface scattering is embedded within a diffusive model of bulk transport, and we show that, for randomly arranged interfaces, the overall system is well described by effective medium theory. Using bulk parameters similar to those of PbTe and a square barrier potential for the interface electron scattering, we identify the interface scattering parameters for which the figure of merit ZT is increased. We find the electronic scattering is generally detrimental due to a reduction in electrical conductivity; however for sufficiently weak electronic interface scattering, ZT is enhanced due to phonon interface scattering.

I. INTRODUCTION

There has been considerable recent interest in utilizing nanostructure to enhance thermoelectric performance [1–4]. A good thermoelectric has scattering mechanisms for phonons and electrons with different features: electron scattering should be strongly energy-dependent, while phonon scattering should simply be strong. Nanostructured materials may provide a route to meeting both requirements [5]. Nanostructure can change a material's basic electronic properties; for example, the inclusion of localized impurity states can enhance peaks in the density of states [6], leading to a stronger energy-dependence of conductivity. Alternatively, nanostructure on a length scale greater than the mean free path does not change the constituent materials' basic electronic properties, but scattering at the interface between material phases changes the bulk composite properties (in this case, "microstructure" may be more apt terminology than "nanostructure"). For example, a mismatch in material density or sound speed generally decreases the phonon conductivity through interface scattering. Additionally, some interfaces provide a potential (*e.g.* a Schottky barrier) which serves as an effective energy filter, transmitting higher energy electrons, while blocking lower energy electrons [7]. The effect of nanostructuring on the thermoelectric figure of merit ZT was systematically studied in Ref. 8, where ZT enhancement was observed for a range of nanocomposite mixing. Refs. [9, 10] provide other examples of ZT enhancement through nanostructuring. Ref. [11] employed both nanostructuring and microstructuring to achieve scattering at varying length scales, and found a large ZT enhancement in PbTe. Previous theoretical works have analyzed in detail either electron [12] or phonon scattering [13] at specific interfaces. Refs. [14] and [15] calculate the effect interface scattering on electron and phonon lifetime in a Boltzmann transport approach, and find the conditions under which this scattering leads to ZT enhancement.

In this work, we employ a linear response model of transport to study a material with randomly arranged interfaces, where the length scale of the material structure is much greater than the mean free path of electrons and phonons. The electronic transport across an interface is calculated with a Landauer approach, while the diffuse mismatch model is used to describe the interfacial phonon transport. The interface resistances are incorporated into bulk transport using effective medium theory. Our model applies to systems in the diffusive regime. Similar work has been done in considering thermal transport in composite materials [16, 17], and the electronic component of thermoelectric transport [18, 19]. In treating both electron and phonon transport, we find that ZT enhancement occurs over a fairly narrow range of material and interface parameters. This reinforces the importance of scattering at multiple length scales, as exemplified in the experiments of Ref. [11], among others. This work also demonstrates the potentially deleterious effect of interface scattering at large length scales. Generally, we find that in this regime of large length scale structure, ZT is enhanced via interfacial phonon scattering, only if the electron scattering is sufficiently weak. The paper is organized as follows: in Sec. II, we give model details, including descriptions of effective medium theory, and the treatment of electron and phonon scattering, in Sec. III, we present results, and conclude in Sec. IV.

II. MODEL

The starting point is the linear response description of transport for the electrical current j and thermal current j_Q [20]:

$$j = -\sigma\nabla V - \sigma S\nabla T \,, \tag{1}$$

$$j_Q = -\kappa\nabla T - \sigma ST\nabla V \,, \tag{2}$$

$$\nabla\cdot j = 0; \nabla\cdot j_Q = 0, \tag{3}$$

where σ is the local electrical conductivity, κ^e (κ^γ) is the electron (phonon) contribution to the total local thermal

conductivity κ ($\kappa = \kappa^e + \kappa^\gamma$) (all thermal conductivities evaluated for zero electric field), S is the thermopower, V is the electrostatic potential, and T is the temperature. The figure of merit ZT is [21]:

$$ZT = \frac{S^2\sigma T}{\kappa - S^2\sigma T}. \quad (4)$$

An ideal thermoelectric has a large power factor $S^2\sigma$, and low phonon thermal conductivity: $\kappa^\gamma \ll \kappa^e$.

To study the thermoelectric properties of a polycrystalline system with randomly arranged interfaces, we imagine discretizing the system into elements with length greater than the mean free path electrons and most heat-carrying phonons (length scales are discussed more fully in the next subsection). We use a random site approach in which sites are randomly assigned as belonging to grain 1 with probability c, or to grain 2 with probability $(1-c)$. In this paper we fix $c = 1/2$. The link between two sites represents a resistor (or conductance), whose value is set by the adjacent site types (see Fig. 1). If both sites belong to the same grain, the resistance is set to $\Delta x/\sigma$, where σ is the bulk conductivity and Δx is the element size. We take Δx to be much greater than the (maximum) mean free path of electrons and phonons. If adjacent sites belong to distinct grains, then an interface resistance is added in series to the bulk resistance (see Appendix B for expressions of transport parameters of elements in series). In the absence of interface scattering, Δx factors out of the problem and is not important. In the presence of interface scattering, Δx is a key model parameter: a small Δx implies a higher interface density, and a more significant effect of the interface scattering. We study the effect of varying Δx later in the paper.

Following this recipe, the probability of an uninterrupted chunk of N identical sites is $(1/2)^N$. This leads to the probability distribution shown in Fig. 1c, where the mean grain size is $2\Delta x$, and the standard deviation of $\sqrt{2}\Delta x$. It should be noted that the grain lengths along different directions are not correlated in this model. This distribution is similar to the commonly used log-normal distribution for grain sizes [22], where $P(g) = \frac{1}{\sqrt{2\pi}sg}\exp\left[-\frac{1}{2}\left(\ln\frac{(g/m)}{s}\right)^2\right]$; here g is the grain size, and m and s are the median and width of the distribution of grain sizes, respectively.

Given an ensemble of configurations, Eqs. (1-3) can be solved directly. We present some numerical results in this work, where we discretize the system into 30^3 sites, and ensemble average so that the statistical error of the effective transport parameters is converged (this typically requires 30 systems). Alternatively, Eqs. 1-3 may be solved semi-analytically using effective medium theory, which we describe in subsection 2.

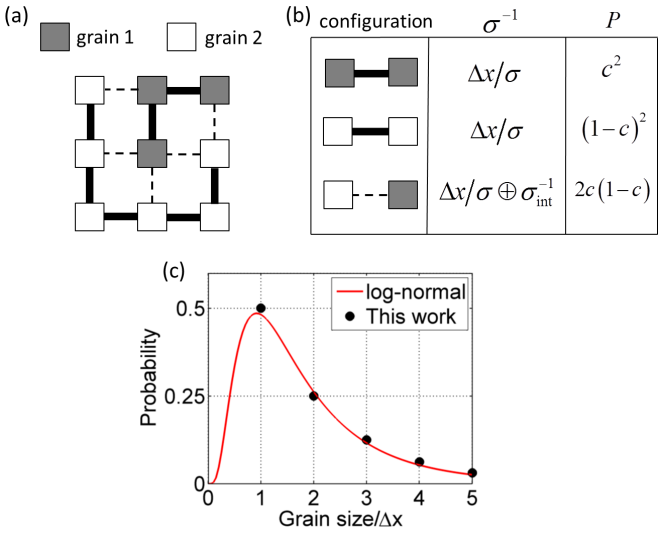

FIG. 1: (a) depicts a typical random site configuration, where the links between sites are set by the adjacent site types. (b) shows the values of resistance for each link type, along with the probability for each link type. Δx is the minimum grain size, and $\Delta x/\sigma \oplus \sigma_{\text{int}}^{-1}$ is the series resistance of $\Delta x/\sigma$ and σ_{int}^{-1}. (c) compares the distribution of grain side lengths generated by this model to a log-normal distribution, with parameters $m = 1.5$ (median), and $s = 0.7$ (width).

1. *Length scales*

The approach described in this paper is applicable to systems with length scale of the material structure greater than the electron and phonon mean free paths. For electrons in a degenerately doped semiconductor, the mean free path for most carriers is between 2 and 5 nm at 300 K [15]. For phonons, the picture is more complicated: The phonon conductivity can have substantial contributions from a wide range of phonon wavelengths, and the mean free path for phonons varies substantially with phonon wavelength. For example, at 300 K Si has 50% contribution to κ^γ from phonons with mean free path greater than 400 nm [23]. This is much greater than the length scales envisioned in this work. The treatment of the effect of nanostructure in this regime of long phonon mean free path can be handled by a modified effective medium theory, as described in Ref. [24]. For materials such as Si and SiGe, where the relevant phonon mean free path is large, nanostructuring has proven to be an effective strategy to improving ZT [9, 10]. On the other hand, for PbTe at 300K, molecular dynamics calculations show that approximately 50% of the conductivity is carried by phonons with mean free path less than 10 nm [25]. In this case, the model described here is more appropriate. Generally, good bulk thermoelectric materials have a small phonon thermal conductivity, and therefore a small phonon mean free path. The approximations used in this work apply more readily to these

materials.

2. effective medium theory

The transport properties of a multi-component, disordered system can be approximated with effective medium theory (EMT). As shown in Ref. 26, the effective medium electrical conductivity σ and total thermal conductivity κ satisfy:

$$\sum_i P_i \left(\frac{\sigma_i - \sigma}{\sigma_i + 2\sigma} \right) = \sum_i P_i \left(\frac{\kappa_i - \kappa}{\kappa_i + 2\kappa} \right) = 0 \ , \quad (5)$$

while the thermopower S is given as:

$$S = 3\kappa\sigma \left(\sum_i P_i \frac{\sigma_i S_i}{(\kappa_i + 2\kappa)(\sigma_i + 2\sigma)} \right) \times \left(\sum_i P_i \left[\frac{\sigma_i\kappa + \sigma\kappa_i + 2\sigma\kappa - \sigma_i\kappa_i}{(\kappa_i + 2\kappa)(\sigma_i + 2\sigma)} \right] \right)^{-1} , \quad (6)$$

where i labels the link type, and P_i is the probability of a link with transport parameter values $\sigma_i,\ \kappa_i,\ S_i$.[27]

3. interface electron scattering

To model electron scattering at a grain boundary, we use a square potential barrier with height V_0 and width w. The physical picture is that each grain boundary creates an interfacial accumulation of carrier traps which become charged, thus forming a potential barrier [29, 30]. To find the interface transport parameters, we start with a Landauer picture of transport, where the interface separate two reservoirs at different chemical potentials and temperatures. The resulting "two-probe" conductance values (denoted with "Landauer" subscript) are given by: $(\sigma_{\text{Landauer}} = \frac{2e^2}{h} L_0,\ (S\sigma)_{\text{Landauer}} = \frac{2ek_{\text{B}}}{h} L_1,\ \kappa^e_{\text{Landauer}} = \frac{2k_{\text{B}}^2 T}{h} L_2)$, where L_j is related to the transmission probability $T(E)$ according to:

$$L_j = \frac{1}{2\pi^2} \int\int d\mathbf{k}_\parallel dE \, (E - E_f)^j \, T\left(E, \mathbf{k}_\parallel\right) \left(\frac{\partial f}{\partial E} \right) , \quad (7)$$

where $\mathbf{k}_\parallel$ is the Bloch wave vector parallel to the interface.

We assume a free electron dispersion: $E = \hbar^2\mathbf{k}^2/2m$. Eq. 7 can be conveniently recast by partitioning the electron energy into components normal and parallel to the interface: $E = E_\perp + E_\parallel = \hbar^2 \left(k_\perp^2 + \mathbf{k}_\parallel^2 \right)/2m$. We note that $d\mathbf{k}_\parallel = 2\pi k_\parallel \left(dk_\parallel \right) = 2\pi m \left(dE_\parallel \right)/\hbar^2$, (here $k_\parallel = |\mathbf{k}_\parallel|$). Finally Eq. 7 is written as:

$$L_j = \frac{m}{\pi\hbar^2} \int\int dE_\parallel dE \, (E - E_f)^j \, T\left(E_\perp\right) \left(\frac{\partial f}{\partial E} \right) . \quad (8)$$

The transmission probability through a square barrier with width w and height V_0 is given by:

$$T(E_\perp) = \left(1 + \frac{4V_0^2}{E_\perp (E_\perp - V_0)} \sin^2 \left(\sqrt{E_b^{-1} (E_\perp - V_0)} \right) \right)^{-1} , \quad (9)$$

where $E_b = \hbar^2/(2m_e w^2)$.

The Landauer conductance (equivalently, the Landauer resistance) includes contributions from the reservoir contact. As discussed in Ref. [31], the bare interface resistance is obtained by, roughly speaking, subtracting off the interface resistance contribution. We discuss this in more detail and provide the expressions for interface transport parameters in Appendix A.

A similar approach is used in Ref. 12 where the carriers' mean free path for backscattering is calculated assuming an infinite number of identical potential barriers. This is then used to estimate the interfacial scattering relaxation time and to determine the transport coefficients using the Boltzmann approach. It can be shown [32] that if a mean free path for backscattering in the Landauer approach is properly defined, and the grains are assumed similar in size, that the Landauer and Boltzmann approaches are consistent with one another. Here we include the effects of interface scattering on the thermoelectric transport within effective medium theory (Eqs. 5-6).

4. interface phonon scattering

We employ the diffuse mismatch model to approximate the phonon scattering at the grain boundary interface [33]. As described in Ref. [34], the diffuse mismatch model for interfacial phonon transport can be formally constructed in similar fashion as the Landauer approach for electrons. According to this model, the phonon interface conductance is:

$$\kappa^\gamma_{\text{DMM}} = \frac{1}{4} \sum_j v_{L,j} \int_0^\infty \alpha_{L,j} \hbar\omega \frac{dN(\omega, T)}{dT} d\omega , \quad (10)$$

where $\alpha_{L,j}$ ($v_{L,j}$) is the transmission probability (velocity) of the phonon incoming from the left side of the interface (j labels the mode), and $N(\omega, T)\, d\omega$ is the number of phonons between ω and $\omega + d\omega$. In the diffuse mismatch model, the transmission probability depends on the ratio of the phonon density of states on the left and right side of the interface. For identical materials, $\alpha = 0.5$. Similar to the electronic interface conductance, the above expression implies a finite conductance even for $\alpha = 1$. Ref. [35] describes how to extract a true interface conductance within the diffuse mismatch model, and shows that for the special case of two identical bulk materials, α is replaced by $\alpha/(1 - \alpha)$ (so that a perfectly transmitting interface has zero interface resistance, as expected). We take the temperature to be greater than the Debye

symbol	quantity	value
m_0	effective mass	0.16 m_e
E_F	Fermi level	0 eV
T	temperature	700 K
v	phonon velocity	1770 m/s
C	heat capactity	1.15×10^6 J/ $\left(\mathrm{m}^3 \cdot \mathrm{K}\right)$
σ	electrical conductivity	3×10^4 $(\Omega \cdot \mathrm{m})^{-1}$
κ	thermal conductivity	3 W/ $(\mathrm{m} \cdot \mathrm{K})$
S	thermopower	150 μV/K
Δx	minimum grain size	100 nm
α	phonon transmission	0.5
w	barrier width	0.3 nm

TABLE I: Default model parameters. The Fermi level is chosen so that the density of carriers at $T = 700\ K$ is $n = 4.3 \times 10^{18}$ cm^{-3}.

temperature, and the above expression reduces to:

$$\kappa^{\gamma}_{\mathrm{DMM}} = \frac{1}{4} v C \left(\frac{\alpha}{1-\alpha} \right) \tag{11}$$

where v is the speed of sound, and C is the heat capacity (at the high temperatures considered here, $C = 3Nk_B$, where N is the atomic density). Unless otherwise specified, we take $\alpha = 0.5$.

III. RESULTS

To clarify the physics underlying the role of interface scattering, we start by evaluating the bare interface conductance, then study a single interface between two grains, and finally consider a medium with a random arrangement of interfaces.

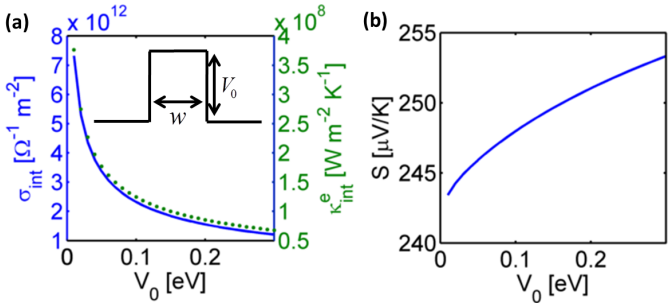

FIG. 2: (a) shows the interface electrical conductance (solid line) the electronic thermal conductance (dotted line) versus barrier height, for fixed barrier width of $w = 0.3$ nm. (b) shows the interfacial thermopower for the same parameters.

Figure 2a shows the electrical and electronic thermal conductance versus potential height, for a fixed barrier width of 0.3 nm, and fixed phonon scattering with $\alpha = 0.5$. The electrical conductance decays rapidly [36], and we note that the Wieddeman-Franz law is approximately satisfied [37]. Figure 2b shows that the thermopower increases with V_0: a higher barrier is a more effective energy filter than a lower barrier. Critically, S_{int} increases more slowly than σ_{int} decreases, so that the benefit of enhanced energy filtering is overwhelmed by the detrimental loss of conductivity. This is not surprising: S is a ratio of transport parameters, so its variation with barrier properties is weak compared to the bare conductance. This means that the power factor $S^2\sigma$ (and therefore ZT) is reduced as electronic scattering increases. This underlies the electronic aspect to all of the ensuing results: the effect of electronic scattering on efficiency is almost entirely negative; the best strategy is simply to minimize its impact.

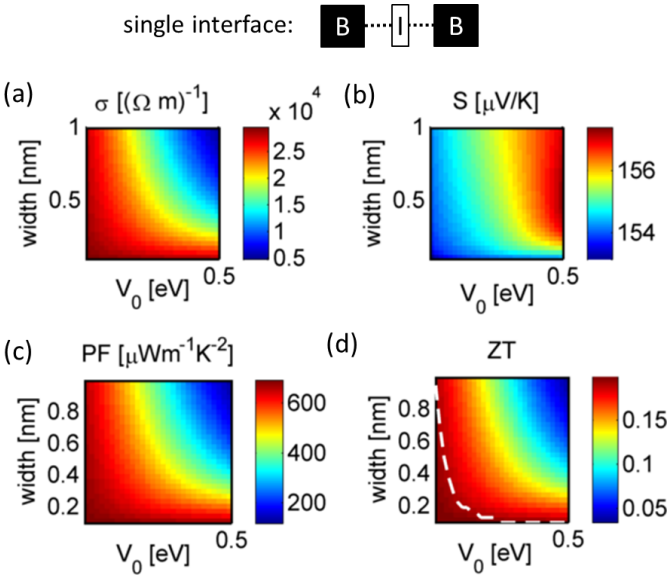

FIG. 3: The transport parameters for a single interface separating two bulk regions, as a function of barrier height and width. The grain size is taken to be $\Delta x = 100$ nm. The bulk values are: $\sigma = 3 \times 10^4\ \Omega^{-1}\mathrm{m}^{-1}$, $S = 150\ \mu$V/K, $PF = 675\ \mu\mathrm{Wm}^{-1}\mathrm{K}^{-2}, ZT = 0.19$. ZT of the system is increased over the bulk value below the white line in (d).

This scenario of reduced power factor due to interface scattering is illustrated using a system as shown in Fig. 3: a single interface between two grains. We take the length of each bulk region to be half a grain size (assumed to be 100 nm), combine the three transport elements in series, as described in Appendix C, and divide by the grain size. Panels (a)-(d) show the conductivity, thermopower, power factor, and ZT value as we vary the electronic barrier properties, keeping the phonon scattering fixed with $\alpha = 0.5$. As before, the thermopower S is weakly dependent on barrier properties, while the electrical conductance σ decreases rapidly for higher and/or wider barriers. The power factor $S^2\sigma$ therefore decreases

from interface scattering. Below the white line of Fig. 3d, ZT is enhanced. Generally, ZT is enhanced due to phonon scattering, whenever electron scattering is sufficiently weak.

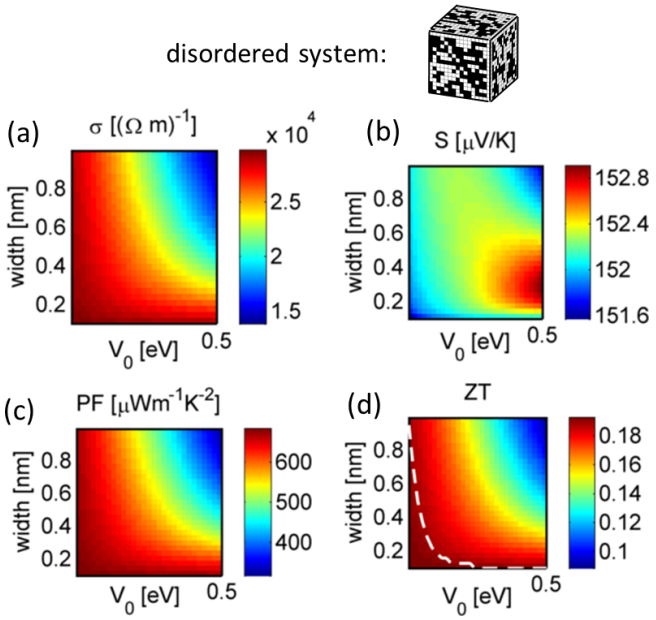

FIG. 4: The transport parameters for a disordered medium, as a function of barrier height and width, as computed using effective medium theory. The same parameters are used as in Fig. 3 (minimum grain size of $\Delta x = 100$nm. The qualitative trend is very similar.

The effect of interface scattering for the disordered medium is qualitatively similar to that of the the single interface. This is shown in Fig. 4, where we again show the conductivity, thermopower, power factor, and ZT value versus interface barrier height and width, for fixed phonon transmission $\alpha = 0.5$. The trends follow those of the single interface, but the conductance and thermopower are less affected in the disordered medium by interface scattering, as compared to the single interface. The net effect on ZT is very similar, however. The similarity between the results shown in Figs. 3 and 4 suggest that the qualitative impact of of interface scattering in a complex, disordered material may be gleaned by the detailed study of just a single interface, with the requisite condition that the length scale of the disorder is much greater than electron and phonon mean free paths.

We next show the range of barrier height and widths which result in ZT enhancement, for different values of bulk conductivity. The solid curve (b) in Fig. 5 corresponds to the white line in Fig. 4(d). Here $\sigma = 3 \times 10^4\ (\Omega \cdot \mathrm{m})^{-1}$ and the bulk ZT is 0.19. For the curve (a) of Fig. 5, the bulk σ is reduced to $1 \times 10^4\ (\Omega \cdot \mathrm{m})^{-1}$, and the bulk ZT is 0.06. Here there is a large set of barrier parameters which lead to ZT enhancement. Contrastly, the curve labeled (c) has a higher bulk $\sigma = 5 \times 10^4\ (\Omega \cdot \mathrm{m})^{-1}$,

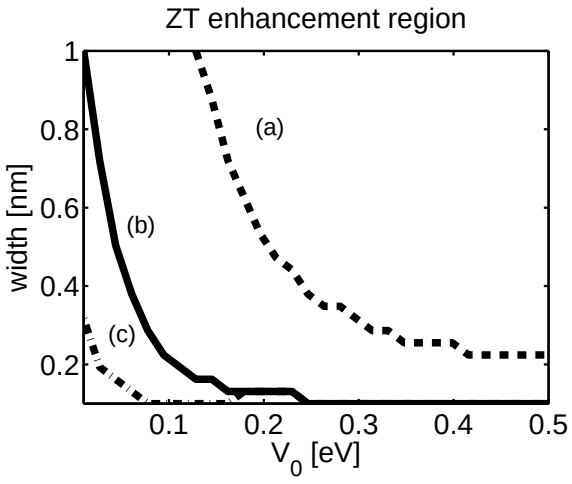

FIG. 5: curves showing region of ZT enhancement for three different values of bulk conductivity σ. The region below each curve represent the interface barrier parameters for which ZT is increased over its bulk value. The curves (a), (b), (c) correspond to $\sigma = (1, 3, 5) \times 10^4\ \Omega^{-1}\mathrm{m}^{-1}$, which yield bulk ZT values of 0.06, 0.19, 0.36, respectively. The percentage enhancement in the three cases is 5 %, 3 %, 1 %.

higher $ZT = 0.36$, and a much more restricted space of ZT enhancement versus barrier parameters. Loosely speaking, these results show that interface scattering can most easily and effectively increase ZT if the bulk material has a low ZT initially.

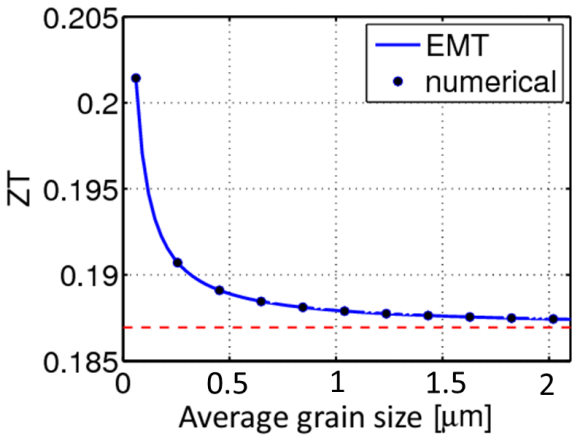

FIG. 6: ZT as a function of the average grain size for a disordered medium, for interface scattering parameters of $w = 0.3$ nm, $V_0 = 0.01$ eV. Solid line is result from effective medium theory, and dots indicate numerical results. The dashed red line indicates the bulk value of ZT.

Figure 6 shows ZT for fixed barrier height of $V_0 = 0.01$ eV and width $w = 0.3$ nm, as a function of the average grain size, using both effective medium theory, and

solving Eqs. (1-3) for an ensemble of randomly chosen systems. (Recall that in our model, the average grain size is twice the minumum grain size; the grain size distribution is shown in Fig. 1(c)). We find almost perfect agreement. Reducing the grain size increases the ratio of interface to bulk scattering, so that the effect of interfaces (be it beneficial or detrimental to ZT) increases as the grain size decreases. We emphasize that there is a lower limit to the grain size for which this model applies, given by the electron and phonon mean free path, as discussed in Section II. Although not explored here, we note that effective medium theory is perfectly suited to describe materials with a distributed set of parameters (*e.g* a distribution of barrier heights), as studied in Ref. 18.

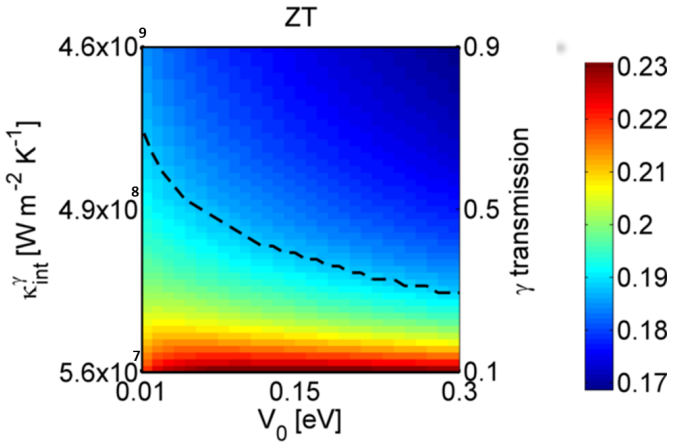

FIG. 7: ZT of disordered medium as a function of interface barrier height for electrons (for fixed barrier width of w = 0.3 nm), and phonon thermal interface conductance. This is related to the averaged phonon transmission probability via the diffuse mismatch model, as indicated on the right hand axis. The region below the black line has a ZT value enhanced over the bulk.

So far, we have assumed that the interface phonon scattering is described by the ideal diffuse mismatch model, for which the transmission probability is 0.5. More sophisticated modeling of phonon transmission through grain boundaries in Si in Ref. [38] shows that this model applies to high energy phonons, but that lower energy phonons transmit more readily through grain boundaries. This suggests that the averaged transmission probability should therefore be larger than 0.5. On the other hand, for phonons with mean free path greater than the grain size, the interfaces will increase their bulk scattering, reducing their contribution to the thermal conductivity. This extra scattering could be mapped into a reduced transmission probability. In any event, we may freely vary the transmission probabilitity, and the effect on ZT is shown in Fig 7. Here we also vary the potential barrier height. For the region below the black line, ZT is increased over its bulk value. We find that: 1. the interface transmission probability must be below 0.7 in order to result in any ZT enhancement, and 2. a higher phonon transmission probability necessitates a lower barrier height for ZT enhancement. This conforms to the overall picture that: interface scattering has a positive impact via phonon scattering, and a negative impact via electron scattering. As the benefits of phonon scattering are reduced (e.g. higher phonon transmission), the system is more susceptible to harmful electron scattering.

IV. CONCLUSION

In this paper, we incorporated interface scattering of electrons and phonons in a model of diffusive bulk transport of disordered thermoelectric materials. We found that electronic scattering was generally detrimental to the overall figure of merit ZT, because of the reduced electronic conductivity. However, for sufficiently weak electron scattering, the phonon scattering present at interfaces can lead to an increased ZT. We find the for a material with parameters similar to those of PbTe at high temperatures, the capacity to increase ZT with grain boundary scattering is rather limited. However, the approach developed here is more widely applicable, and, given the energy-dependent transmission coefficients of electrons and phonons, can be straightforwardly applied to any other material. Moreoever, we find that the qualitative effect of interface scattering in a disordered material can be understood in terms of its effect for a single interface. This should facilitate experimental and theoretical studies of ZT enhancement in microcomposites, as the transport properties of a single interface are more easily quantified as compared to a random arrangement of interfaces.

V. ACKNOWLEDGEMENTS

A.P. acknowledges support under the Cooperative Research Agreement between the University of Maryland and the National Institute of Standards and Technology Center for Nanoscale Science and Technology, Award 70NANB10H193, through the University of Maryland.

[1] J. R. Sootsman, D. Y. Chung, and M. G. Kanatzidis, Angew. Chem. Int. Ed., **48**, 8616 (2009).
[2] G. Chen, M. S. Dresselhaus, G. Dresselhaus, J. P. Fleurial, and T. Caillat, Int. Mater. Rev. **48**, 45 (2003).
[3] T. C. Harman, P. J. Taylor, M. P. Walsh, and B. E. LaForge, Science **297**, 2229 (2002).

[4] J. P. Heremans, C. M. Thrush, and D. T. Morelli, Phys. Rev. B **70**, 115334 (2004).
[5] M. G. Kanatzidis, Chem. Mater. **22**, 648 (2010).
[6] J. P. Heremans, V. Jovovic, E. S. Toberer, A. Saramat, K. Kurosaki, A. Charoenphakdee, S. Yamanaka, and G. J. Snyder, Science **321**, 554 (2008).
[7] J. Martin, L. Wang, L. Chen, and G. S. Nolas, Phys. Rev. B **79**, 115311 (2009).
[8] P. F. P. Poudeu, J. DAngelo, H. Kong, A. Downey, J. L. Short, R. Pcionek, T. P. Hogan, C. Uher, and M. G. Kanatzidis, J. Am. Chem. Soc. **128**, 14347 (2006).
[9] G. Joshi, H. Lee, Y. Lan, X. Wang, G. Zhu, D. Wang, R. W. Gould, D. C. Cuff, M. Y. Tang, M. S. Dresselhaus, G. Chen, and Z. Ren, Nano Lett. **8**, 4670 (2008).
[10] X. W. Wang, H. Lee, Y. C. Lan, G. H. Zhu,3, G. Joshi, D. Z. Wang, J. Yang, A. J. Muto, M. Y. Tang, J. Klatsky, S. Song, M. S. Dresselhaus, G. Chen, and Z. F. Ren, App. Phys. Lett. **93**, 193121 (2008).
[11] K. Biswas, J. He, I. D. Blum, C.-I Wu, T. P. Hogan, D. N. Seidman, V. P. Dravid and M. G. Kanatzidis, Nature **489**, 414 (2012).
[12] A. Popescu, L. M. Woods, J. Martin, and G. S. Nolas, Phys. Rev. B **79**, 205302 (2009).
[13] G. Chen, Phys. Rev. B **57**, 14958 (1998).
[14] S. V. Faleev and F. Léonard, Phys. Rev. B **77**, 214304 (2008).
[15] A. J. Minnich, H. Lee, X. W. Wang, G. Joshi, M. S. Dresselhaus, Z. F. Ren, G. Chen, and D. Vashaee, Phys. Rev. B **80**, 155327 (2009).
[16] Ce-Wen Nan, R. Birringer, D. R. Clarke, and H. Gleiter, J. App. Phys. **81**, 6692 (1997).
[17] Ce-Wen Nan, R. Birringer, Phys. Rev. B **57**, 8264 (1998).
[18] A. A. Snarskiia, A. K. Sarychevb, I. V. Bezsudnovc, and A. N. Lagarkovb, Semiconductors, Vol. **46**, 659 (2012).
[19] F. Gather, C. Heiliger and P. J. Klar, J. Phys. Condens. Matter **23**, 335301 (2011).
[20] The equation of continuity for heat current is generally $\nabla \cdot j_Q = j \cdot \nabla V + j_Q \cdot \nabla T/T$. In linear response the right-hand-side of this equation can generally be ignored. The full nonlinear version with heating was solved in the numerical calculation, and was found to agree with the results when heating is neglected.
[21] G. D. Mahan and J. 0. Sofo, Proc. Natl. Acad. Sci **93**, 7436 (1996).
[22] Espiau de Lamaëstre and H. Bernas, Phys. Rev. B **73**, 125317 (2006).
[23] A. S. Henry and G. Chen, J. Comput. Theor. Nanosci. **5**, 141 (2008).
[24] A. Minnich and G. Chen, App. Phys. Lett. **91**, 073105 (2007).
[25] B. Qiu, H. Bao, G. Zhang, Y. Wu, and X. Ruan, Comp. Mat. Sci. **52**, 278 (2012).
[26] I. Webman, J. Jortner, and M. H. Cohen, Phys. Rev. B **16**, 2959 (1977).
[27] This is the Bruggeman symmetric form of effective medium theory, which is appropriate to use as we make no *a priori* assumptions as to the geometry of the disorder [28].
[28] A. H. Clark, Thin Solid Films **108**, 285 (1983).
[29] R. E. Jones, Jr. and S. P. Wesolowskia, J. App. Phys. **56**, 1701 (1984)
[30] C. H. Seager, J. Appl. Phys. **52**, 3960 (1981).
[31] U. Sivan and Y. Imry, Phys. Rev. B **33**, 551 (1986).
[32] C. Jeong, R. Kim, M. Luisier, S. Datta, and M. Lundstrom, J. Appl. Phys. **107**, 023707 (2010).
[33] E. T. Swartz, R. O. Pohl, Rev. Mod. Phys. **61**, 605 (1989).
[34] C. Jeong, PhD Thesis (appendix B), Purdue University (2012).
[35] S. Simons, J. Phys. C **7**, 4048 (1974).
[36] Naively one expects the conductance to decay exponentially with the barrier height V_0. However, for the very thin barrier used, and the high temperature of the electron distribution, we observe that the conductance decreases approximately as $1/\sqrt{V_0}$.
[37] G. D. Mahan and M. Bartkowiak, App. Phys. Lett. **74**, 953 (1999).
[38] P. K. Schelling, S. R. Phillpot, and P. Keblinski, J. App. Phys. **95**, 6082 (2004).
[39] S. Kirkpatrick, Rev. Mod. Phys. **45**, 574 (1973).

VI. APPENDIX

A. Thermoelectric interface transport

Here we offer a brief flavor of the reasoning involved in deriving the interface conductances within a Landauer picture, and refer the reader to Ref. [31] for a detailed explanation and discussion. The bare Landauer conductance includes the contributions from the reservoir contact, which we want to exclude in order to determine the interface conductance. The interface conductance is proportional to the difference in chemical potential immediately on either side of the interface. The transmission and reflection coefficients T and R can be used to relate the chemical potential on either side of the interface with the reservoir chemical potentials. For zero temperature, this relation is found by expressing the density $n(\mu)$ (which is a function of the chemical potential μ) in terms of reservoir chemical potentials (μ_L and μ_R), and separately expressing the density n in terms of the the local chemical potential ($\mu_{L/R \text{ of interface}}$), and finally setting both expressions equal:

$$n(\mu_{L \text{ of interface}}) = (1+R)\, n(\mu_L) + T n(\mu_R) \quad , (12)$$
$$n(\mu_{R \text{ of interface}}) = (1+R)\, n(\mu_R) + T n(\mu_L) \quad . (13)$$

Eqs. (12-13) determine the chemical potential drop immediately across the interface, thereby determining the interface conductance. For finite temperature, a similar relation between local and reservoir temperatures is derived by considering the entropy to the left and right of the interface (the relation above is additionally modified at finite temperature). The final interface conductance values are written in terms of the following integrals:

$$L_j = \frac{1}{2\pi^2} \int\int d\mathbf{k}_\parallel dE\, (E-E_f)^j\, T(E) \left(\frac{\partial f}{\partial E}\right), \quad (14)$$
$$A_j = \frac{1}{2\pi^2} \int\int d\mathbf{k}_\parallel dE \frac{(E-E_f)^j}{\sqrt{E-E_T}} \left(\frac{\partial f}{\partial E}\right), \quad (15)$$

$$B_j = \frac{1}{2\pi^2}\int\int d\mathbf{k}_\parallel dE \frac{(E-E_f)^j}{\sqrt{E-E_T}} R(E)\left(\frac{\partial f}{\partial E}\right), \quad (16)$$

where E_f is the Fermi energy, $f(E,E_f)$ is the Fermi-Dirac distribution function, and $\mathbf{k}_\parallel$ is the Bloch wave vector parallel to the interface. The interface transport parameters are finally given by:

$$\sigma_{\rm int} = \frac{L_0(B_2A_0 - B_1A_1) + L_1(A_1B_0 - A_0B_1)}{B_0B_2 - B_1^2} \quad (17)$$

$$(S\sigma)_{\rm int} = \frac{L_0(B_2A_1 - B_1A_2) + L_1(A_2B_0 - A_1B_1)}{B_0B_2 - B_1^2} \quad (18)$$

$$(S\sigma)'_{\rm int} = \frac{L_1(B_2A_0 - B_1A_1) + L_2(A_1B_0 - A_0B_1)}{B_0B_2 - B_1^2} \quad (19)$$

$$\kappa^e_{\rm int} = \frac{L_1(B_2A_1 - B_1A_2) + L_2(A_2B_0 - A_1B_1)}{B_0B_2 - B_1^2} \quad (20)$$

where the two thermoelectric transport coefficients are: $j = -(S\sigma)\nabla T$, $j_q = -(S\sigma)'T\nabla V$. Usually these two coefficients are equal, by Onsager's principle. However in this case, they may differ, as discussed in Ref. [31]. In practice, we find the two quantities differ by less than 2% for the cases we have studied.

B. Combining thermoelectric transport elements

For two components in series with different transport parameters, Eqs. (1-3) can be solved to find the effective transport parameters of the lumped circuit element. In this case it's convenient to work with $P \equiv S\sigma$. In terms of individual elements transport parameters $(\sigma_1, \kappa_1, P_1)$ and $(\sigma_2, \kappa_2, P_2)$, the lumped element parameters $(\sigma_{12}, \kappa_{12}, P_{12})$ are given by:

$$\sigma_{12} = D\left[(\kappa_1+\kappa_2)\sigma_1\sigma_2 - \left(P_2^2\sigma_1 + P_1^2\sigma_2\right)T\right] \quad (21)$$

$$\kappa_{12} = D\left[(\sigma_1+\sigma_2)\kappa_1\kappa_2 - \left(P_2^2\kappa_1 + P_1^2\kappa_2\right)T\right] \quad (22)$$

$$P_{12} = D\left[\kappa_1\sigma_1P_2 + \kappa_2\sigma_2P_1 - P_1P_2(P_1+P_2)T\right] \quad (23)$$

where $D = (\sigma_1+\sigma_2)(\kappa_1+\kappa_2) - (P_1+P_2)^2T$. Eqs. 21-23 are used to combine interface and bulk transport parameters when there is an interface present.